The Effect of Surfactants on Nitric Oxide Solid Sensors Prepared By Sol-Gel

Jair Pereira de Melo Junior[1]*, Carlos Alberto Brunello[2], Rondinelli Donizetti Herculano[3], Marcelo Bighetti Toniollo[1], Hugo Machado Sanchez[1], Carlos F.O Graeff[4]

[1]Departament of Biophysics, Faculty of Medicine, University of Rio Verde, Rio Verde, Brazil, [2]Departament of Physics, FFCLRP, São Paulo University - USP, Ribeirão Preto, Brazil,[3]Departament of Bioprocesses and Biotechnology, Faculty of Pharmaceutical Sciences, São Paulo State University - UNESP, Araraquara, Brazil; [4]Departament of Physics, School of Sciences, São Paulo State University - UNESP, Bauru, Brazil;
CorrespondingAuthor:Jair Pereira de Melo Junior

--**ABSTRACT**---

The effects of surfactants (CTAB, SDS, Triton X100 and Pluronic® F127) on the structure and performance of nitric oxide (NO) solid sensor are reported. Surfactants decreases the fragility of the solid sensors, specially CTAB and Triton. The drying time was optimized to 30 min. The most intense EPR signals were obtained with the surfactants Triton, SDS and CTAB at a concentration of 12 mM and F127, 4,6 mM. The signal-to-noise ratio improves significantly with the use of surfactants. The NO diffusion was estimated in a qualitative way through the NO trapping time, the best performance was obtained using F127 and SDS. Signal saturation occurred after 10 min. The highest mobility of the NO-Fe^{2+}-$DETC$ complex was found in the SDS and F127 sensors evidenced by line shape analysis. For the solid-state sensor the detection limit without any surfactant was 10 μM, whereas using F127, 2μM.

KEYWORDS-*Nitric Oxide, Sol-gel, EPR,Sensor,Surfactants*

I.   INTRODUCTION

Nitric oxide (NO) is afree radical species synthesized by the amino acid L-arginine extremely important in many biological systems [1-5]. It functions as messenger molecule that regulates physiologic functions, including vasodilatation, respiration, immune response and apoptosis [6], besides participating in carcinogenic processes [7]. Since its discovery as an endothelium-derived relaxing factor (EDRF) [8], this molecule has attracted the interests of researchers from different areas. NO has a cytotoxic effect to bacterial lipopolysaccharide (LSP) [9], in the central nervous system the neuroprotection versus neurotoxicity depends on NO concentration [10].

Numerous researchers have been engaged in its detection [11], however due to its short half-life and its high reactivity, the detection and direct quantification of NO in real time is a challenge [12,13]; the detections are in general indirect, measuring nitrite (NO_2^-) and nitrate (NO_3^-) [14-16]. Electron paramagnetic resonance using spin traps is promising in the detection and quantificationof NO [15,17-19], including real-time imaging [20,21]. Sensors in solid state are preferable due to the limitations of Electron Paramagnetic Resonance (EPR) measurements of liquids. There is a large number of NO traps in use, among them dithiocarbamate (DTCs) and derivatives[22].

Iron complexes with DTCs derivatives are among the most important spin-trap agents in use, due to the strong NO interaction with the Iron complex forming nitrosyl complexes such as NO-Fe^{2+}-$DETC$.
In previous works we presented a solid sensor capable of NO quantification using FeDETC in a silicon oxide matrix prepared by sol-gel[24], in natural rubber latex[25] and in a poly (2,6-dimethyl-1,4-phenylene oxide) (PPO) matrix [26]. Sol-gel materials have been used in many different applications such as enzyme [27] or antibodies trapping [28], and inorganic catalysts [29,30]. Solid matrices, mesoporous thin films and organized pores with controlled sizes, can be produced using surfactants [31-34]. The structure of the materials used in the solid sensors production for NO detection and quantification is important specially in what concerns the pores that are formed during the synthesis process.
In this work, we report the effect of surfactants on sensors prepared by sol-gel. The sensing was made using EPR. The surfactants used were SDS, Triton X100, CTAB and F127.

II. MATERIALS AND METHODS

NO was generated in the following way: $NaNO_2$ 10 mM (250 mL), deionized water (750mL) and $Na_2S_2O_4$ (145mg) were mixed in an Eppendorf tube of 1.5mL. The final concentration in the solution was 2.0 mM (saturation). In some cases, the solution was diluted with Milli-Q water to obtain NO in different concentrations (0 to 2.0 mM).

For the experiments with the surfactants CTAB, Triton X100 and SDS, a sol-gel (SG) solution was prepared mixing under stirring, 4 mL of Tetraethyl Orthosilicate (TEOS), 4mL of ethanol and 1.45 mL of H_2O. The pH was adjusted to 2 with HCl 2M. Then the solution was submitted to ultrasound for 10 min, with subsequent magnetic stirring for 90 min, 1mL of DMF was added and the solution was stirred magnetically for more 30 min.

At the same time, a Fe^{2+}-DETC (20 mg of $FeCl_3$ + 67 mg of DETC + 10 mL of DMF + magnetic stirring for 60 min) was added to the gel under constant stirring until the color of the solution has changed from a dark (almost black) to light green-yellow. The Fe^{2+}-DETC solution and the gel were mixed separately inside the Eppendorf tubes in an aliquot of 1:3 v/v (Fe^{2+}- DETC:SG). The surfactants were added to the Fe^{2+}-DETC: SG solutions in a way to obtain a final solution (Fe^{2+}-DETC: SG + surfactants), with concentrations ranging from 6 to 16mM in either solid or liquid state.

The surfactant solution was prepared through the dissolution of thesalts in aqueous medium in the following way: 0.1442 g SDS (99%, PM = 288.38g/mol), or 0.1822 g CTAB (99%, PM = 364.46 g/mol) or 0.3224 g Triton (99%, PM = 646.86 g/mol) were added in a 25 mL Becker to obtain an aqueous solution of 100 mM.Deionized water was used in the procedure.

The solid sensors with different quantities of surfactants (6 to 16 Mm) were prepared, putting 60 mL of the final solution (Fe^{2+}-DETC:SG + surfactants) inside capillary tubes of ~100mL capacity. The sensors mass was measured by the difference between the capillary mass + SG after drying through a precision analytical balance. The surfactants final concentration in the SG was obtained by dilution from 0 to 16 mM. The Fe^{2+}-DETC/SG was kept in a volume of 1:3[24]. The capillaries containing the SG were submitted to a thermal treatment under constant temperature (30ºC) in a drying oven. The drying time was ~12 h; the result was a porous solid with a cylinder format inside the capillaries.

SG solution using F127 was prepared by the following procedure: 4.27 mL TEOS was put in a Becker and kept under stirring with 1.5 mL HCl 0.055M. Afterwards, 22.81 mL ethanol was added and 1.14 g F127 was poored slowly under constant stirring. The final solution F127-SG (4.6 mM) was kept under stirring for 1h until complete dissolution. This was necessary due to the low solubility (10%) of F127 in aqueous medium compared to the others (Triton X, CTAB and SDS). The solutions were prepared by dilution of the original F127-SG solution (saturated at 4.6mM) with concentrations from 0.35 mM to 4.6 mM. Immediately before measurements this solution was mixed with Fe^{3+}-DETC.

A reference solution was prepared referred as DMF-solution, in the following way: 10 mL Fe^{3+}DETC (20 mg $FeCl_3$ + 67mg DETC + 10 mL DMF) was exposed to NO. 10 different solutions containing NO in concentration that varied from 0 to 2 mM were obtained and measured using a 150 µL capacityflat cell.

NO trapping was made by inserting the capillaries containing the solid sensors, as described before, in a sodium dithionite solution that acts as a strong reducer for 30 min. Than the capillaries were taken out and inserted in a saturated solution of sodium nitrite ($NaNO_2$) containing sodium dithionite for a period that varied from 0 to 60 min. The same procedure was done for the undried sensors (SG solution).
For the NO-Fe^{2+}-DETC EPR detection in SG solution flat cells of 150 µL capacity were used at room temperature. The experiment was done using different concentrations of NO.

EPR measurements were done on a Varian-E4 band X spectrometer coupled with a Lock-in amplifier EG&G 7260, to a HEWLETT PACKARD 5350B Microwave Frequency Counter and adapted to be remotely controlled by a microcomputer. The EPR spectrometer operated with field modulation of 100 kHz, amplitude modulation of 0.4mT, time constant 500ms, microwaves power of 20 mW, scan field of 20mT, scan time of 2min with accumulation of two scans. For the EPR measurements, the dry capillaries were inserted in EPR quartz tubes while the solutions through a flat cell. The estimated signal intensity error is 10%.

The specific area and volume of the pores were determined by the Brunauer-Emmett-Teller (BET) method and the distribution of the pores volume was obtained by the Barrett, Joyner, and Halenda (BJH) method. The equipment used was a Micromeritics ASAP 2020. The experiments were done using approximately 0.3g of the solid sensors.

III. RESULT AND DISCUSSION

As already mentioned, although NO is a free radical, it cannot be directly measured using EPR, it must be stabilized by trapping [17]. In our previous work, the detection limit using similar sensors was found to be 10 µM, incompatible with the detection of NO in physiological levels, of around 1.0 µM. One great advantage of this sensor is that it operates at room temperature.

One of the main restrictions of sol-gel glasses is their fragility [24]. This problem in our sensors was solved with the use of surfactants. The materials obtained became less fragile and the drying time was also reduced by half; without surfactants our sensors needed 24 h drying, with surfactants about 12 hours. The drying temperature was also reduced from 50°C to 30°C. Decreasing the processing temperature is important since DETC degrades as the temperature is raised making the formation of the complex with iron more difficult [35].

A good solid sensor must have, among others features, great sensibility, a net of pores well-distributed and connected to facilitate NO diffusion and active traps. Thus, it is important to know if FeDETC is formed in ferric or ferrous state since just the $NO-Fe^{2+}DETC$ is paramagnetic ($S = \frac{1}{2}$) [38].

In the synthesis process of the solid sensors when $FeCl_3$ and DETC are mixed the solution becomes dark demonstrating that the complex formed is ferric (Fe^{3+}-DETC). The solution $SG-Fe^{3+}$-DETC (with or without surfactant) goes through a drying process so that the volatile solvents can be removed promoting hydrolysis and condensation until the final product is formed. After drying, the solid is put in contact with a NO solution in a reducing medium (dithionite) for trapping thus generating predominantly $NO-Fe^{2+}$-DETC. It is worth to remind that NO can be trapped by Fe^{2+}-DETC or Fe^{3+}-DETC. The ferric complex $NO-Fe^{3+}$-DETC is diamagnetic with a characteristic light-yellow color and, therefore, does not show an EPR signal [38].

Figure 1 shows the normalized EPR signal intensity as a function of surfactant concentration. There is a clear maximum for all surfactants used at 12 mM. The EPR signal intensity was divided by the sensor mass prior to normalization.
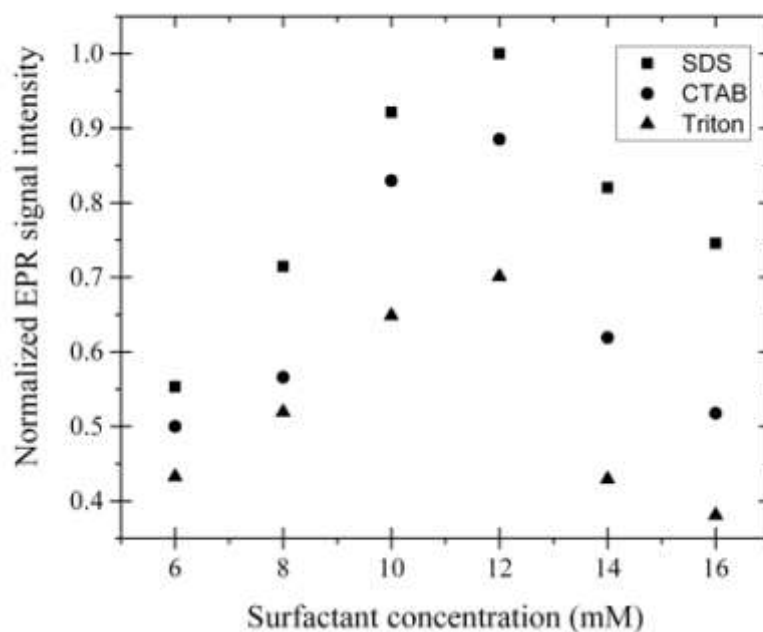

Figure 1. Normalized EPR signal intensity of the $NO-Fe^{2+}$-DETC sensors as a function of surfactants concentration (SDS, CTAB and Triton) between 6 and 16mM. The solid sensors were prepared in the same conditions. The experiment was made at room temperature.

For surfactants concentration higher than 14mM the sensors became gelatinous and difficult to manipulate since it adhered to the capillary tube. For F127, not shown, the signal increases linearly from 0.35mM to 4.6mM.

In Figure 1 it is shown that as the surfactant concentration increases, the intensity of the EPR signal increases proportionally up to 12mM independent of the surfactant used. Above 12mM the signal decreases and the solids lose stiffness and become gelatinous. In concentrations higher than 12 mM the sensors do not dry completely.

The solid sensors prepared without surfactants have a dark coloration that indicates the presence of Fe^{3+}-DETC [38]. When in the NO solution the coloration changes to light yellow indicating the formation of $NO-Fe^{3+}$-DETC (S=0). But the sensors prepared with surfactants have a colorless coloration (Fe^{2+}-DETC) which changes to light green in the NO solution; signalizing the formation of the paramagnetic complex, $NO-Fe^{2+}$-DETC [38].

The sensors porosity was evaluated by BET. Table 1 shows the main parameters obtained and associated values. Apparently, pores size does not influence the EPR signal intensity. As can be seen there is no significant difference in pore size in all sensors evaluated.

Table 1. Solid sensors analysis using the BET method.

Surfactants	Pores Vol. cm^3/g	Pores width (nm)	Pores diameter (nm)	Adsorption m^2/g	Surface area m^2/g
SDS	0.38	2.98	3.96	204.10	501.22
CTAB	0.38	2.70	3.84	202.74	554.39
TRITON	0.46	3.06	4.12	289.00	583.48
F127	0.39	3.02	3.98	206.20	503.13

In Figure 2, the EPR signal intensity as a function of sensor immersion time is presented. As can be seen a maximum is reached after 10 min for all surfactants used. The signal intensity for F127 is larger compared to the other surfactants, reaching intensities about 4 times higher than Triton and CTAB in the first 2 min.
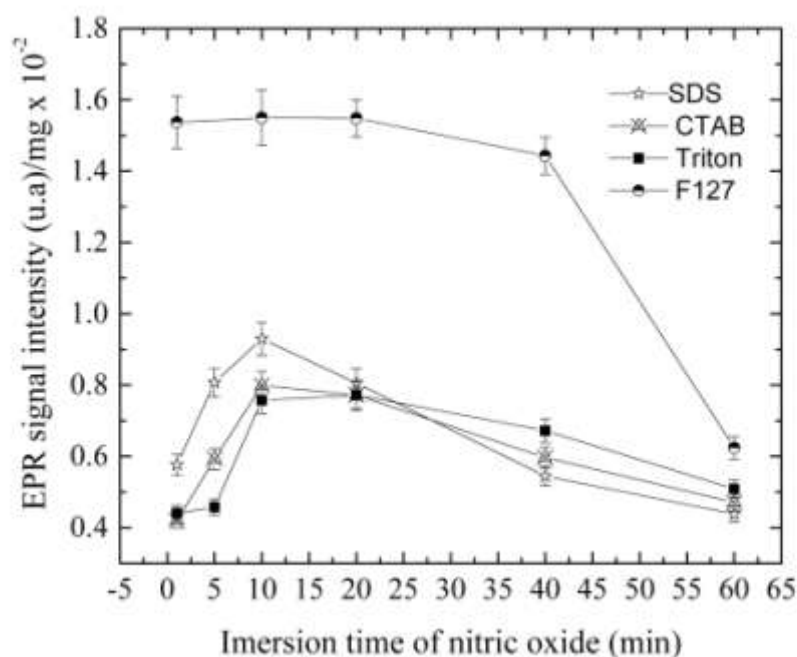

Figure 2.EPR signal intensity as a function of immersion time for the sensors prepared with the surfactants SDS, CTAB and Triton, both with concentration of 12mM and F127 with a concentration of 4.6 mM.

The sensors porosity was evaluated qualitatively through the trapping time, see Figure 2. The signal from the F127 sensor reached intensities about 4 times higher than Triton and CTAB in the first 2 min, indicating that the structure of the sensors produced with F127 allows NO to diffuse more easily and that there is a higher density of active Fe^{2+}-DETC complexes available in the pore network compared to other surfactants.

With the exception of F127, all other sensors have similar trapping dynamics. The structural analysis by BET (Table 1), does not show a significant difference in surface area or pore volume, in other words, apparently, there is no clear relation between the amplitude of the EPR signal with the pore diameter or volume. However, the addition of the polymeric surfactant F127 lead to the formation of more homogeneous mesopores structure, which could be attributed to formation of larger mixed micelles and stronger interactions between protonated PEO chains and the silica species [39]. Pluronic F127 is a PEO-PPO-PEO (PEO: polyethylene oxide) PPO: polypropylene oxide copolymer with an amphiphilic nature that self-aggregates in aqueous solutions to form spherical micelles with hydrophobic PPO cores surrounded by hydrophilic PEO coronas [40].

The EPR spectra can be seen in Figure 3. The EPR signals of the solid sensors prepared with the F127 resemble the line shape in gel (colloidal state). As expected, the EPR signal could only be observed using the reducing agent Na$_2$S$_2$O$_4$.
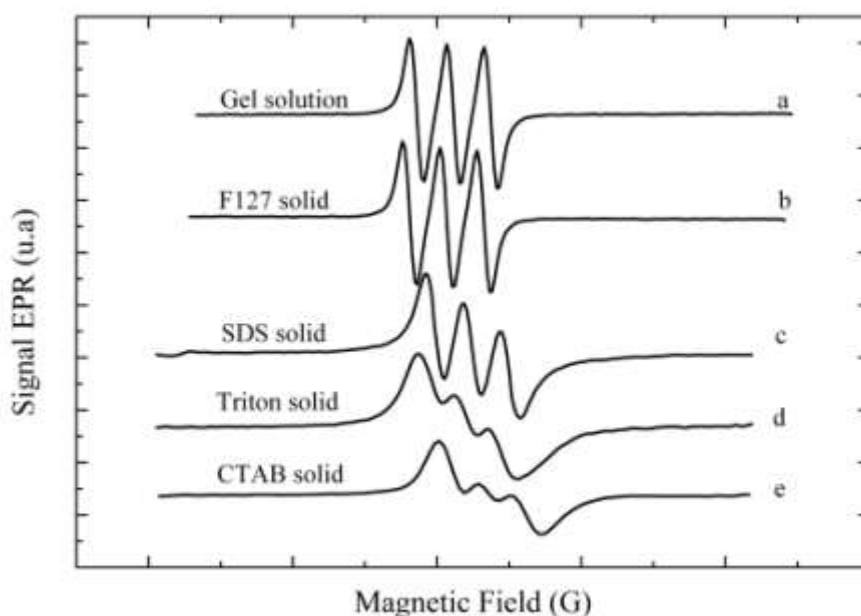
Figure 3. EPR signal of the complex NO-Fe^{2+}-DETC in different matrices: (a) inside a gel without surfactants before drying (colloidal state); (b,c,d,e) in the matrix using the four surfactants, F127, SDS, Triton and CTAB.

From Figure 3, the line shape of the signal obtained in the colloidal solutions SG (liquid) is similar to the F127 and SDS is in an intermediate shape. This is a clear indication that the NO-Fe complex is more fluid inside F127, which may reflect a better pore connectivity. This can explain the increase in the detection limit found in these surfactants in relation to the Triton and CTAB. The better connectivity could also explain that the sensors prepared with F127 and SDS presented a green color similar to the ones in the colloidal solution, while Triton and CTAB the sensor was light yellow with some dark parts indicating that in these sensors there is NO-Fe^{2+}-DTEC (green, EPR active), NO- Fe^{3+}-DETC (light yellow, EPR inactive) and Fe^{3+}-DETC (dark color, NO free) [38]. All sensors were reproducible, all the tests were made in triplicate, with similar results.

In Figure 4 the EPR signal as a function of NO concentration is presented for different matrixes. Notice that for all sensor a linear dependence is observed, the best results were obtained using F127.
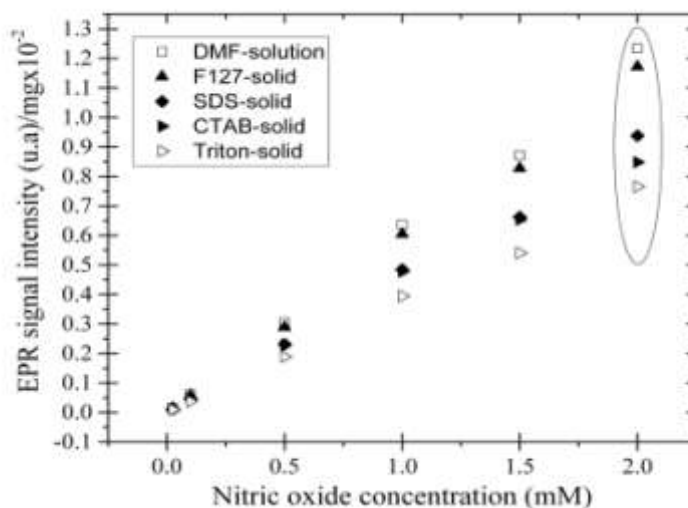

Figure 4. EPR signal intensity for different NO concentrations and sensors in solid state, SG-F127 and DMF-solution.

In the figure 4 we can compare the results obtained from the surfactants in the sensors in solid state with the results in DMF-solution. The reference curve is the DMF-solution, prepared as it is described in the experimental section. For the low NO concentration (25μM) all the sensors in solid state and DMF-solution presented the same intensity of the EPR signal, however, as the NO concentration increases the sensors answers change in relation to the surfactant used. In 2 mM the EPR signal intensity of the sensor in the solid state prepared with the Triton represents 62% of the signal intensity obtained in the DMF-solution. This indicates that during the drying process the numbers of Fe^{2+}-DETC decreased when compared with the DMF-solution. The presence of the gel also affects the quantity of the active complexes. The same thing can be seen with the SDS and CTAB. Referring to the F127 in solid state the intensity of the EPR signal is practically the same when compared with the DMF-solution. In this way we can infer that the number of the Fe^{2+}-DETC complexes actives are almost the double in the sensor prepared with the F127 in comparison to the Triton, with NO in 2mM concentration.

IV. CONCLUSION

We have presented the effect of some surfactants on the EPR signal of the NO-Fe^{2+}-DETC obtained from a solid sensor prepared by the SG method. The process of the sensor synthesis was improved with the use of the surfactants reducing the drying temperature to ~30º. Different concentrations were used and the ideal concentration that connects intense signals and good mechanical resistance was of 12mM, above this the sensors become gelatinous and adherent to the capillaries surface, making harder the NO trapping. The maximum intensity of the EPR signal was obtained for a NO trapping time of 10 min for all the surfactants, however, in 2 min the NO molecules were already complexed. The sensor sensibility in the solid state increases 5 times with the F127. The detection limit with the sensor in the solid sensor was of 2μM with the F127 (physiological level < 1μM). The DETC can be degraded during the synthesis process or affected by pH. There is a similarity as the line shape of the EPR signals between the sensors in the solid state and in the colloidal state for the F127 and SDS. Apparently, there was no influence of the pores size of the sensors in the NO trapping, we inferred that the surfactants, in some way, increase the density of the Fe^{2+}-DETC complexes in the sensors.

ACKNOWLEDGEMENTS

REFERENCE

[1]. Habib S, Ali A. Biochemistry of nitric oxide. Indian Journal of Clinical Biochemistry. 2011;26(1):3–17.
[2]. Phaniendra, A, Jestadi, DB, &Periyasamy, L. Free Radicals: Properties, Sources, Targets, and Their Implication in Various Diseases. Indian Journal of Clinical Biochemistr. 2015;30(1),11–26.
[3]. Buerk, DG, Barbee, KA, Jaron, D. Nitric Oxide Signaling in the Microcirculation. Critical Reviews in Biomedical Engineering. 2011;39(5):397–433.
[4]. Oleson BJ, Broniowska KA, Naatz A, Hogg N, Tarakanova VL, Corbett, JA. Nitric Oxide Suppresses β-Cell Apoptosis by Inhibiting the DNA Damage Response. Molecular and Cellular Biology. 2016;36(15): 2067–2077.
[5]. Mutchler SM, Straub AC. Compartmentalized nitric oxide signaling in the resistance vasculature. Nitric Oxide: Biology and Chemistry. Official Journal of the Nitric Oxide Society. 2015;49(4):8–15.
[6]. Brüne B. Nitric oxide: NO apoptosis or turning it ON? Cell Death Differ. 2003;10(8):864–869.
[7]. Muntané J, De la Mata M. Nitric oxide and cancer. World J Hepatol. 2010;2(9):337–344.
[8]. Ignarro LJ, Byrns RE, Buga GM, Wood KS. Endothelium-Derived Relaxing Factor From Pulmonary Artery and Vein Possesses Pharmacologic and Chemical Properties Identical to Those of Nitric Oxide Radical. Circulation Research. 1987;61(2):866-879
[9]. Kröncke KD, Fehsel K, Kolb-Bachofen V. Nitric oxide: cytotoxicity versus cytoprotection- how, why, when, and where? Nitric Oxide. 1997;1(2):107–120.
[10]. Calabrese V, Mancuso C, Calvani M, Rizzarelli E, Butterfield DA, Stella AMG. Nitric oxide in the central nervous system: neuroprotection versus neurotoxicity. Nat Rev Neurosci. 2007;8(10):766–775.
[11]. Yang Y, Qi PK, Yang ZL, Huang N. Nitric oxide based strategies for applications of biomedical devices. Biosurface and Biotribology. 2015;1(3):177–201.
[12]. Kelm M. Nitric oxide metabolism and breakdown. BiochimBiophys Acta. 1999;1411(2-3):273-289.
[13]. Bryan NS, Grisham MB. Methods to detect nitric oxide and its metabolites in biological samples. Free Radic Biol Med. 2007;43(5):645–657.
[14]. Giustarini D, Rossi R, Milzani A, Dalle-Donne I. Nitrite and Nitrate Measurement by Griess Reagent in Human Plasma: Evaluation of Interferences and Standardization. Methods in Enzymology. 2008;440(6):361–380.
[15]. Tsikas D. Methods of quantitative analysis of the nitric oxide metabolites nitrite and nitrate in human biological fluids. Free Radic Res. 2005;39(8):797–815.
[16]. Romitelli F, Angelo S, Chierici E, Pitocco D, Tavazzi B, Maria A, et al. Comparison of nitrite/nitrate concentration in human plasma and serum samples measured by the enzymatic batch Griess assay, ion-pairing HPLC and ion-trap GC – MS: The importance of a correct removal of proteins in the Griess assay. J Chromatogr B. 2007;851(1-2):257–267.
[17]. Kleschyov AL, Wenzel P, Munzel T. Electron paramagnetic resonance (EPR) spin trapping of biological nitric oxide. J Chromatogr B. 2007;851(1):12–20.
[18]. Cammack R, Shergill JK, Inalsingh VA, Hughes MN. Applications of electron paramagnetic resonance spectroscopy to study

interactions of iron proteins in cells with nitric oxide. Spectrochimica Acta Part A: Molecular and Biomolecular Spectroscopy. 1998;54(14):2393–2402.

[19].   Sheu F, Zhu W, Fung PCW. Direct Observation of Trapping and Release of Nitric Oxide by Glutathione and Cysteine with Electron Paramagnetic Resonance Spectroscopy. Biophysical Journal. 2000;78(3):1216–1226.

[20].   Sharma R, Seo J-W, Kwon S. In Vivo Imaging of Nitric Oxide by Magnetic Resonance Imaging Techniques. J Nanomater. 2014;2014(2):2-13.

[21].   Yoshimura T, Kato N. In vivo and ex vivo EPR spectroscopy and imaging of endogenously produced nitric oxide under physiological and pathophysiological conditions. EPR in the 21st Century. 2002;403–411.

[22].   Vanin AF, Liu X, Samouilov A, Stukan RA, Y JLZ. Redox properties of iron dithiocarbamates and their nitrosyl derivatives : implications for their use as traps of nitric oxide in biological systems. Biochimica et Biophysica Acta. 2000;1474(3):365–377.

[23].   Kleschyov AL, Wenzel P, Munzel T. Electron paramagnetic resonance (EPR) spin trapping of biological nitric oxide. J Chromatogr B. 2007;851(1-2):12-20.

[24].   Melo JP, Biazzotto JC, Brunello CA, Graeff CFO. Solid state nitric oxide sensor prepared by sol-gel entrapment of iron-diethyldithiocarbamate in a siloxane matrix. J Non Cryst Solids. 2004;348(4):235–239.

[25].   Herculano RD, Tzu LC, Silva CP, Brunello CA, Queiroz AAA de, Kinoshita A, Graeff CFO. Nitric oxide release using natural rubber latex as matrix. Mater Res. 2011;14(3):355–359.

[26].   Herculano RD, Brunello CA, Jr JPM, Martins M, Borges FA, Chiavacci LA, et al. Novel Solid State Nitric Oxide Sensor Using Siloxane-Poly (Oxypropylene) (PPO). Materials Sciences and Applications. 2013;4(2):683–688.

[27].   Momeni N, Ramanathan K, Larsson P-O, Danielsson B, Bengmark S, Khayyami M. CCD-camera based capillary chemiluminescent detection of retinol binding protein. Anal Chim Acta. 1999;387(1):21–27.

[28].   Gun J, Lev O. Sol-gel derived, ferrocenyl-modified silicate-graphite composite electrode: Wiring of glucose oxidase. Anal Chim Acta. 1996;336(1–3):95–106.

[29].   Salimi A, Compton RG, Hallaj R. Glucose biosensor prepared by glucose oxidase encapsulated sol-gel and carbon-nanotube-modified basal plane pyrolytic graphite electrode. Anal Biochem. 2004;333(1):49–56.

[30].   Zhao X-M, Xia Y, Whitesides GM. Fabrication of three-dimensional micro-structures: Microtransfer molding. Adv Mater. 1996.;8(10):837–840.

[31].   Torchilin VP. Structure and design of polymeric surfactant-based drug delivery systems. J Control Release. 2001;73(2–3):137–172.

[32].   Naik SP, Yamakita S, Ogura M, Okubo T. Studies on mesoporous silica films synthesized using F127, a triblock co-polymer. Microporous Mesoporous Mater. 2004;75(1–2):51–59.

[33].   Antunes FE, Gentile L, Rossi CO, Tavano L, Ranieri GA. Gels of Pluronic F127 and nonionic surfactants from rheological characterization to controlled drug permeation. Colloids Surf B Biointerfaces. 2011;87(1):42–48.

[34].   Valverde G, Macedo JG, Cruz D, Zink JI, Hernández R. Photoconductivity in mesostructured thin films. Journal of Sol-Gel Science and Technology. 2003;26(1-3):605–608.

[35].   Faassen E Van, Vanin A. NO trapping in biological systems with a functionalized zeolite network. Nitric Oxide. 2006;15(3):233–240.

[36].   Li Y, Xu R, Bloor DM, Holzwarth JF, Wyn-Jones E. The Binding of Sodium Dodecyl Sulfate to the ABA Block Copolymer Pluronic F127 (EO 97 PO 69 EO 97): An Electromotive Force, Microcalorimetry, and Light Scattering Investigation. Langmuir. 2000;16(26):10515–10520.

[37].   Li Y, Xu R, Couderc S, Bloor DM, Wyn-Jones E, Holzwarth JF. Binding of sodium dodecyl sulfate (SDS) to the ABA block copolymer pluronic F127 (EO97PO69EO97): F127 aggregation induced by SDS. Langmuir. 2001;17(1):183–188.

[38].   Vanin AF, Kubrina LN, Faassen E Van. Reduction enhances yields of nitric oxide trapping by iron – diethyldithiocarbamate complex in biological systems. Nitric Oxide. 2007;16(1):71–81.

[39].   Esquena J, Nestor J, Vílchez A, Aramaki K, Solans C. Preparation of mesoporous/macroporous materials in highly concentrated emulsions based on cubic phases by a single-step method. Langmuir. 2012;28(33):12334–12340.

[40].   Basak, R, Bandyopadhyay, R. Encapsulation of hydrophobic drugs in pluronic F127 micelles: Effects of drug hydrophobicity, solution temperature, and pH. Langmuir. 2013; 29(13):4350–4356.